IOSR Journal of Applied Chemistry (IOSR-JAC)
e-ISSN: 2278-5736.Volume 17, Issue 5 Ser. 1 (May 2024), PP 43-58
www.iosrjournals.org

Cola Acuminata Dye Extract: Computational Modeling For Corrosion Inhibition In Acidic Medium

Samson Adehuga Omogbehin[1,2], Emmanuel Folorunsho Olasehinde[1]
Matthew Ayorinde Adebayo[1] Jamiu Mosebolatan Jabar[1]
[1] *Department Of Chemistry, The Federal University Of Technology, Akure, Ondo State, Nigeria*
[2] *Department Of Science Laboratory Technology, Federal Polytechnic, Ile Oluji, Ondo State, Nigeria*

Abstract
This study investigated the potential of a dye extract from the Cola acuminata seeds to inhibit corrosion of mild steel in Hydrochloric acid (1M HCl). A combined approach using experiments and theoretical calculations (quantum chemistry) was employed. Weight loss, electrochemical techniques, and computer modeling were used to assess the extract's effectiveness. Adsorption and thermodynamic properties were examined to understand how the extract interacts with the metal surface. Increasing the extract concentration significantly improved its ability to prevent corrosion. Inhibition efficiency decreased as temperature increased. This suggests the extract needs more energy to function effectively at higher temperatures. Positive ΔH^{0} values indicate the corrosion inhibition process absorbs heat (endothermic). The extract readily sticks (adsorbs) to the metal surface, as shown by the negative ΔG_{ads} values. The adsorption process follows this common model for describing how molecules form a single layer on a surface. Analysis of electrical properties revealed the extract acts through a combined mechanism. Computational calculations predicted Myricetin, a specific component within the extract, to have the strongest inhibitory properties. The close match between theoretical predictions and experimental results highlights the power of quantum chemistry in designing corrosion inhibitors.

Keywords: *Corrosion, Mild Steel, Hydrochloric Acid, Myricetin, Corrosion Rate*

Date of Submission: 21-05-2024 Date of Acceptance: 31-05-2024

I. Introduction

Mild steel's versatility makes it a go-to material in engineering. From building frames and bridge trusses to machinery components, screws, weapons, and car parts, you'll find mild steel playing a crucial role in countless applications. The combination of user-friendliness, strong mechanical performance, and efficient production processes makes these materials a compelling choice [1]. Mild steel, also known as plain- carbon steel is inexpensive and has good properties that allow it to be used for a variety of applications, making the steel vulnerable to corrosion attack.

Among the most effective tools for preventing corrosion damage are corrosion inhibitors [2].

Corrosion inhibitor is one that, when introduced in small amount to a given environment, slows down the rate at which metals exposed to it corrode. Corrosion inhibitors slow down the chemical reactions that cause metal to break down in corrosive environments. Corrosion inhibitors stick to the metal surface, affecting the layer of charged particles surrounding it, which can slow down corrosion. Most industrial corrosion inhibitors are organic molecules containing elements like oxygen, sulfur, and nitrogen. These molecules often have special chemical bonds (pi bonds) and ring structures that help them cling to metal surfaces [3]. Organic dyes, known for their vibrant colors, hold promise in preventing corrosion. The same features that give them color – atoms like oxygen, nitrogen, and sulfur, along with specific chemical structures – also make them likely to stick to metal surfaces, creating a protective layer [4]. *Cola acuminata* (CA) has been the subject of intensive phytochemical study and chemical component isolations. These studies have revealed the presence of several groups, including tannins, alkaloids, flavonoids, anthraquinones, which contain atoms like O and N and functional groups that can help corrosion inhibition [5]. *Cola acuminata* extract has been studied for its potential to prevent mild steel corrosion in acidic conditions [6] Information regarding Quantum Chemical Modeling of *Cola acuminata's* and Corrosion Inhibition specifically remains scarce.

II. Materials And Methods

Preparation and Characterization of Dye Extract of *Cola acuminata* (CA)

The seeds of *Cola acuminata* were cleaned to remove any contaminants. They were ground to powder, sieved, and stored in an airtight container for 21 days. 2 L of 50% ethanol was used to dissolve 1 kg of the ground sample and kept for 3 days. [7].

Sample analysis

The chemical phytochemical makeup of the CA dye was analyzed extract using established methods [8, 9]. UV/Visible spectrophotometer (model Genesys 10 S) was used to examine the colors that the extract absorbs, focusing on light wavelengths between 200 and 800 nanometers (nm). Additionally, an Agilent Technologies FTIR spectrometer was used to identify the types of chemical bonds (functional groups) present in the dye. This analysis provided a detailed fingerprint of the dye chemical structure at a resolution of 8 cm^{-1},scanning a range of 600 cm^{-1} to 4000 cm^{-1}.

Corrosion inhibition studies

Preparation of mild steel

The compositions of the mild steel employed for analysis are: Fe=99.11, Mn=0.359, C=0.149, Cr =0.055, S=0.059, and Ni= 0.048. The metal strips (coupons) were first smoothed by hand using silicon carbide paper. They were then meticulously cleaned with distilled water to remove any dirt. Finally, to ensure a completely oil-free surface, they were degreased with acetone and ethanol, and left to dry naturally in a special container (desiccator) that removes moisture from the air. Using mild steel of dimension 22 mm x 18 mm x 2 mm coupons, the sample weights were obtained using an electronic weighing balance. The experiment employed double-distilled water, and each reagent used in the study was graded analytically [10].

Corrosive environments and inhibitor preparation

To create a corrosive testing environment, a 1.0 M hydrochloric acid solution was prepared by carefully diluting concentrated hydrochloric acid (36.5%) with distilled water. Precisely measured amounts of the extract was then added to this 1.0 M HCl solution to create inhibitor solutions. These inhibitor solutions had different concentrations, ranging from 0.2 to 1.2 grams per liter (g/L).

Weight-loss method

Pre-weighed strips of mild steel were dipped into a solution of 1.0 M hydrochloric acid for three hours. The acid solution contained different amounts of *Cola acuminata* extract. The tests were carried out at various temperatures ranging from 303 to 333 Kelvin K. After three hours, the strips were removed from the acid solution. To remove any remaining corrosion products, they were dipped in a sodium hydroxide (NaOH) solution, followed by cleaning with acetone and distilled water. Finally, the strips were dried completely and weighed again to determine how much weight they had lost due to corrosion. The experiment was repeated three times (triplicate) to ensure accuracy. The average weight loss from these tests was then used to calculate several important factors: the corrosion rate (how fast the metal was corroding), the effectiveness of the inhibitor (percentage inhibition efficiency), and the extent to which the inhibitor covered the metal surface (surface coverage). Equations 1, 2, and 3 as described by (Olasehinde *et al)* [10]

C.R = (1)

Where w = change in weight in g

A = Area in Cm^2

t = Time in hour

% I.E = I - x 100 (2)

and weight loss with and without inhibitor

Ɵ =1- (3)

The test was repeated at 313K, 323K and 323K.

Electrochemical Studies

The experiment used a special three-part container (electrochemical cell) connected to an advanced instrument (electrochemical workstation) from Ivium. Inside the cell, three electrodes played specific roles: a platinum counter electrode, a reference electrode called a saturated calomel electrode (SCE), and the mild steel sample itself, which acted as the working electrode. A small electrical current was gradually applied to the working electrode, sweeping it from negative to positive voltage (cathodically to anodically) relative to its starting voltage (Open Circuit Potential, OCP). The rate of this change was very slow, at 1 millivolt per second (mV/s).This process generated potentiodynamic current-potential curves. All the voltage measurements were referenced to a specific electrode (SCE) for consistency. The same metal sample was used for both the EIS test

(which measures how the material responds to small electrical disturbances) and the polarization measurements (which involve applying a range of voltages) without any additional cleaning between the tests. The EIS test used a small alternating voltage (±10 mV) at various frequencies (20 kHz to 200 Hz) to assess the material's resistance to corrosion [11].

Corrosion efficiency (IE%) will be calculated based on the analysis of the polarization plots using the following equation.

$$IE\% = 1 - \left(\frac{i_{corr}}{i^{o}_{corr}}\right) \times 100\% \quad (4)$$

Based on the measurements, a graphs (Nyquist and Bode plots) was obtained that can be used to calculate percent efficiency (IE%) , which indicates how effective the corrosion inhibitor is

$$IE = \left(\frac{R_{ct} - R^{\circ}_{ct}}{R_{ct}}\right) \times 100\%, \quad (5)$$

where R_{ct} and R^{o}_{ct} represent transfer resistance with and without inhibitor concentrations [11].

Surface morphology

scanning electron microscope (SEM) was used to examine the surfaces of the mild steel strips in great detail. The SEM works in a v

acuum and uses a beam of electrons with an energy of 15 kV to create high-resolution images. Additionally, Energy Dispersive X-ray spectroscopy (EDX) was used to identify the specific elements present on the surfaces of the strips.

GC-MS and HPLC ANALYSIS

The TG dye extract was analyzed by Gas Chromatography-Mass Spectrometry (GC-MS) using Agilent 8860A model for component identification. Further analysis was performed using High-Performance Liquid Chromatography (HPLC) with a variable wavelength detector.

Quantum Chemical Calculations:

The Hartree-Fock Density Functional Theory (HF-DFT) with the Becke 3 Lee Yang Parr (B3LYP) method and a 6-31G* basis set within the Spartan '14 VI.1.4 program software was used to perform quantum chemical studies on the corrosion inhibitors.

III. Results And Discussion

Phytochemical analysis

Cola acuminata dye extract's phytochemical examination reveals the following compounds: tannins, phenols, flavonoids, and alkaloids. Studies reveal that the majority of green inhibitors are made up mostly of phenols, tannins, and alkaloids [12].

Table 1: Phytochemical analysis of CA Dye Extract

Parameter	Observation
Alkaloids	+++
Flavonoids	++
Saponins	+
Tannins	++
Phenols	+++

UV-Vis spectroscopy

The CA dye extract showed two absorption peaks around 230 and 340 nanometers (nm), indicating the presence of aromatic chromophores, which are light-absorbing molecules characteristic of dyes. These peaks could be due to flavonoids or their derivatives, as these compounds typically absorb light in the range of 230 to 400 nm. This finding aligns with research by Mabasa *et al*. [13]. The absorption spectra of flavonoids and phenolic substances are influenced by the presence of aromatic and other cyclic rings in their molecular structures [14].

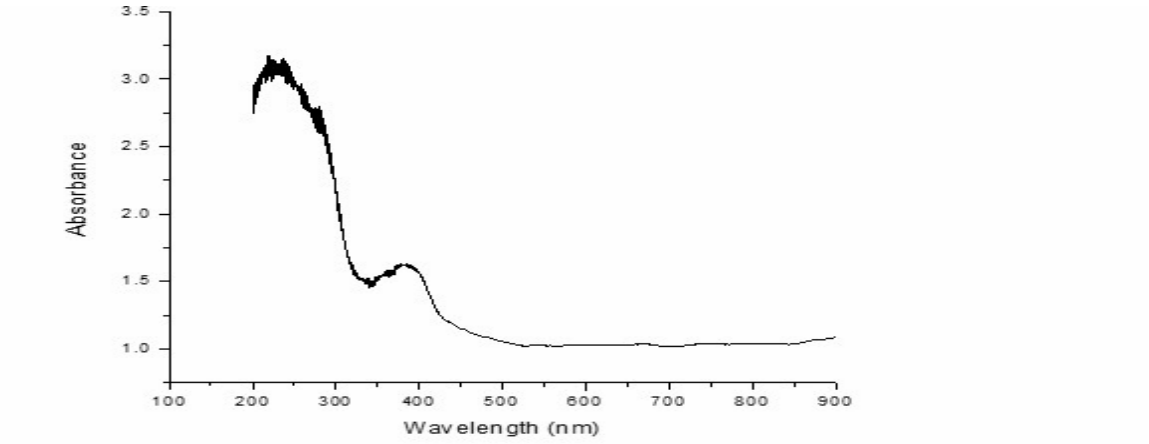

Fig 1 : UV–Vis absorption spectrum of CA dye

FT-IR Analysis

FT-IR analysis of the CA dye extract (Figure 2) revealed the presence of functional groups with wavenumbers ranging from 3294.96 cm^{-1} to 812.56 cm^{-1}. The FT-IR spectrum of the dye extract shows absorption bands between 3294.96 cm^{-1} and 3268.97 cm^{-1}, indicating either N-H stretching of an amine or O-H stretching of an alcohol. The peak between 2929.68 cm^{-1} and 2855.14 cm^{-1} corresponds to C-H bending, while the peak between 1733.21 cm^{-1} and 1625.11 cm^{-1} suggests C=C or C=O stretching vibrations" The dye according to findings, comprise O–H, C=O,C=C, N- H and C–H) atoms in functional groups that satisfy the requirements of a typical corrosion inhibitors [15-17].

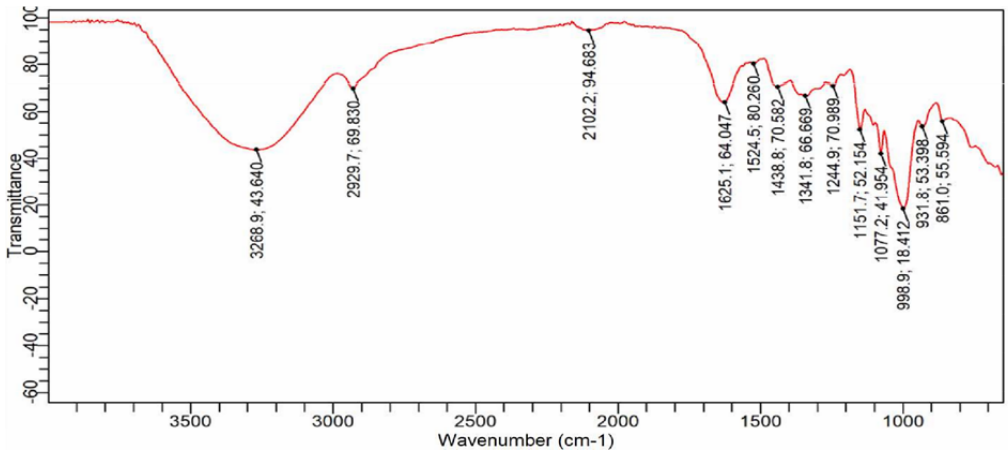

Fig 2: FTIR spectrum of CA dye

Corrosion inhibitory studies

The influence of CA dye concentration and temperature on the corrosion of mild steel in 1 M HCl solution was investigated. Experiments were conducted at various temperatures: 303 K, 313 K, 323 K, and 333 K Figure 3 clearly demonstrates the CA dye inhibitor's effectiveness in reducing the corrosion rate of the metal sample in the acidic medium. This is evident from the significantly higher corrosion rate observed in the blank solution compared to the solution containing the inhibitor. It was discovered that the corrosion rate of the steel sample increased with temperature and decreased with an increase in CA dye inhibitor concentrations [18]. Studies have demonstrated that the corrosion rate of mild steel is not constant and can be significantly affected by factors like inhibitor concentration and temperature

The addition of crude dye resulted in lower corrosion rates, indicating its ability to hinder (retard) mild steel corrosion. This effect is likely due to the presence of heteroatoms and π-electron systems within the dye molecules. These features are known to enhance the dye's adsorption onto metal surfaces and other adsorbents [3,19].

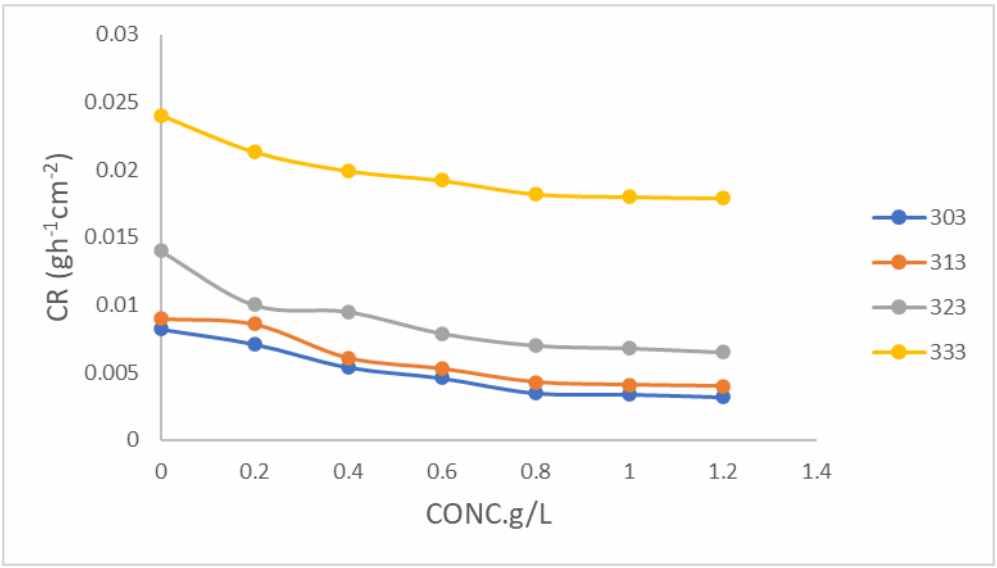

Fig. 3: Corrosion Rate of mild Steel in 1M HCL in presence and absence of CA dye

Inhibitor efficiency

Figure 4 presents the inhibition efficiencies (% IE) of the CA dye inhibitor on the corrosion of the metal sample in the acidic solution. It was shown that the (%IE) decreased with rising temperatures and increased with increases in inhibitor concentration. As the temperature rises, the inhibitory efficiency actually decreases, suggesting that the extracts adsorb to the metal surface by a physical adsorption process [20]. This is in line with previous results found in the literature [4,21]. The decline in effectiveness of dye extracts with temperature is typical of most inhibitors from plant biomass. It is thought that some of the phytochemicals included in the CA dye extract, such as tannins, flavonoids, alkaloids, and polyphenols, contribute to its efficacy. These molecules have heteroatoms (N, S, and O) that can bind to iron surface to create complexes that serve as a shield from ions that can cause corrosion [22]. The efficacy of the dye extracts rose as concentration increased, suggesting that increasing concentration may lead to improved inhibitory efficiency [4].

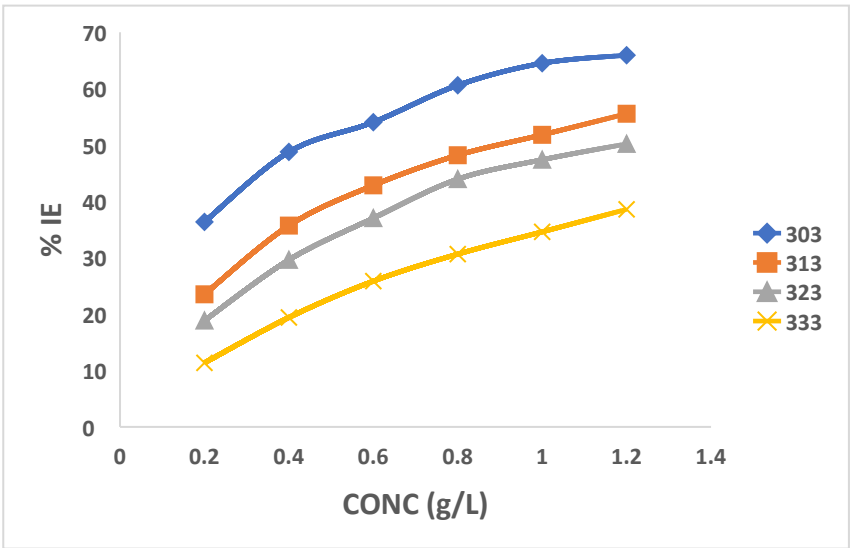

Fig 4: Inhibition efficiency of CA Dye

Thermodynamics Studies

The Arrhenius equation (Ln CR = -Ea / RT + ln A) was employed to calculate the activation energy (Ea) for mild steel dissolution in 1.0 M HCl solution at various temperatures. This calculation was performed both with and without the addition of CA dyePlotting ln(C) versus 1/T resulted in linear graphs (Fig. 5a). The slopes of these lines, which are equal to -Ea/R, were then used to calculate the activation energy (Ea) for the process. Table 2 shows that the activation energies for corrosion in solutions containing the CA dye inhibitor are higher compared to the solution without the inhibitor. This increase in activation energy suggests that the CA

dye likely functions through a physical adsorption mechanism [23]. The higher activation energies (Ea) observed in the presence of the inhibitor (Table 2) correspond to a larger energy barrier for the metal dissolution process. This increased barrier hinders the reaction and supports the effectiveness of CA as a corrosion inhibitor, as reported in [23].The formation of a thin film on the metal surface by the CA dye likely acts as a physical barrier, hindering both the movement of molecules (mass transfer) and the energy transfer needed for corrosion to occur. This increased energy barrier, reflected in the higher activation energies observed (Table 2), supports the conclusion that physical adsorption is the primary mechanism for CA's inhibitory effect, as suggested in [24]. Furthermore, the observed trend of decreasing inhibition efficiency with increasing temperature aligns with the notion that higher temperatures can weaken the physical adsorption of the inhibitor layer [24]. The entropy (ΔS*) and enthalpy (ΔH*) of activation for mild steel corrosion in 1.0 M HCl solution at various CA dye concentrations were determined using plots of ln(CR/T) versus 1/T (Fig. 5b). The slopes of these linear plots correspond to -ΔH*/R, and the intercepts correspond to ln(R/Nh) + ΔS*/R. These values were then used to calculate the activation enthalpy and entropy, which are presented in Table 2. The positive values of activation enthalpy (ΔH*) observed in Table 2 indicate that the dissolution of metal in the presence of the CA dye inhibitor is an endothermic process. This means the process absorbs heat, making it less favorable and potentially explaining the slower corrosion rate. Interestingly, the activation entropy (ΔS*) values are negative for both inhibited and uninhibited solutions (Table 2). This negative entropy suggests an ordered transition state for the hydrogen gas evolution reaction, possibly influenced by the interaction between the metal surface and the CA molecules as reported in [16].

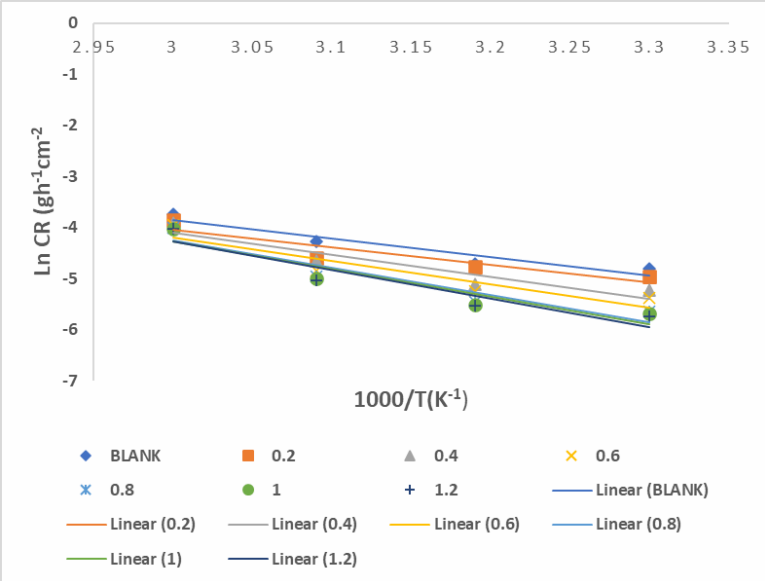

Fig. 5(a): Arrhenius plot for different concentration of CA dye and blank for weight loss methods

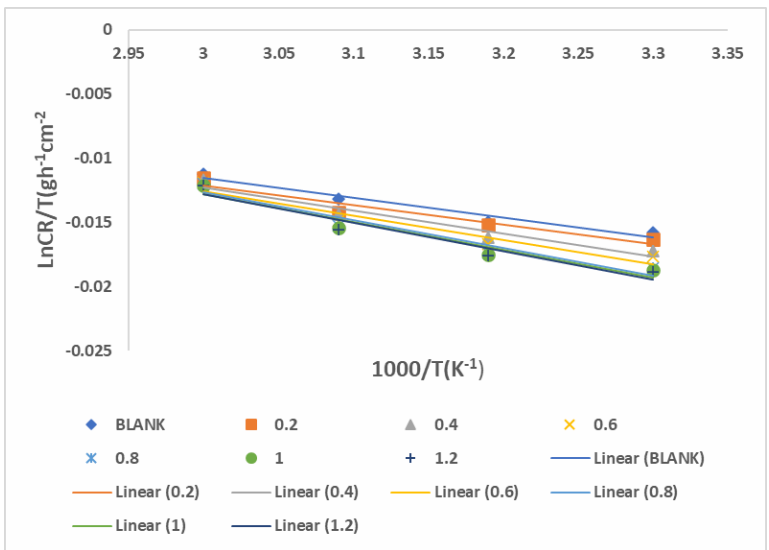

Fig. 5(b): Transition state plot for different concentration of CA dye and blank for weight loss method

Table 2: Thermodynamic activation parameters for the absence and presence of various concentrations of CA dye

CONCENTRATION (gL^{-1})	ACTIVATION ENERGY E_a (KJ mol^{-1})	ENTALTY ΔH^0 (KJ mol^{-1})	ENTROPY ΔS^0 (J $mol^{-1}K^{-1}$)
Blank	**29.71**	**27.10**	**-189.33**
0.2	**30.45**	**27.82**	**-189.18**
0.4	**36.11**	**33.53**	**-187.47**
0.6	**39.77**	**37.05**	**-186.41**
0.8	**45.63**	**43.04**	**-184.62**
1.0	**46.24**	**43.57**	**-184.29**
1.2	**47.66**	**45.16**	**-183.98**

Adsorption Isotherm

Adsorption isotherms explain how organic molecules (adsorbates) cling to a metal surface (adsorbent) at a given temperature. These graphs show the relationship between the amount of the organic molecule that accumulates on the surface and its concentration in the surrounding environment. For the analysis of mild steel corrosion in this study, the Langmuir isotherm model yielded the best match to the experimental results This isotherm assumes a single layer of adsorbate molecules on the metal surface, with no interaction between them. The provided equation ($\Delta G°_{ads}$ = -RT ln(55.5K)) allows us to calculate the standard free energy of adsorption ($\Delta G°_{ads}$) using the Langmuir isotherm. Here, R represents the universal gas constant and T is the absolute temperature (in Kelvin) The calculated standard free energy of adsorption ($\Delta G°_{ads}$) values, presented in Table 3, are all less negative than -40 kJ/mol. This observation suggests that the adsorption of inhibitor molecules on the metal surface likely occurs via physisorption (physical adsorption). Physisorption is generally characterized by $\Delta G°$ads values less negative than -40 kJ/mol, as referenced in [25].

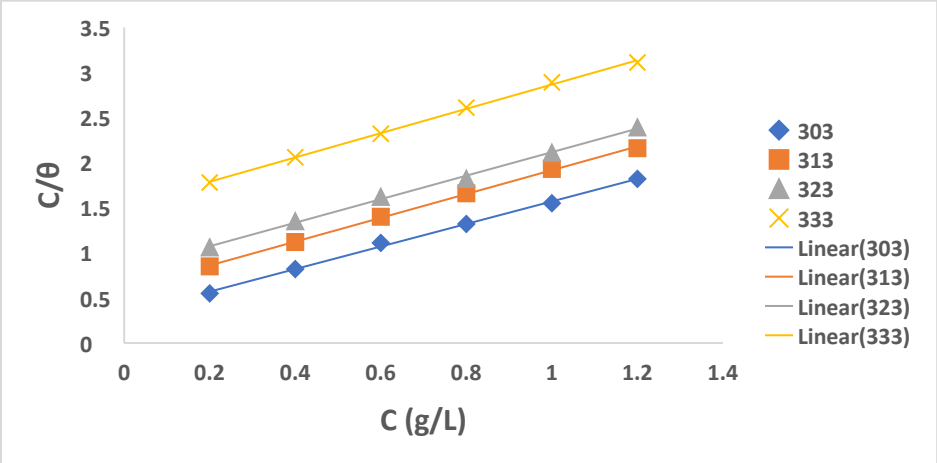

Fig. 6: Langmuir adsorption isotherms for CA dye at different concentrations by weight loss method

Table 3: Calculated parameters of Langmuir isotherm for CA dye in 1.0 M HCl at different temperatures

Temperature(k)	R^2	K_{ads}	Slope	$\Delta G°_{ads}$
303	0.997	3.54	1.20	-13.27KJ
313	0.964	1.93	1.29	-12.94KJ
323	0.999	1.55	1.30	-11.96KJ
333	0.950	0.85	1.33	-10.66KJ

Electrochemical studies

Potentiodynamic polarization

Table 4 summarizes various corrosion parameters obtained from polarization measurements, including cathodic and anodic Tafel slopes (β_c and β_a), corrosion potential (E_{corr}), and corrosion current (I_{corr}), along with their corresponding inhibition efficiencies. Figure 7 illustrates the influence of the extract on the polarization curve.

The results consistently demonstrate that adding the studied compound significantly reduces cathodic current densities, indicating a strong influence on the hydrogen evolution reaction at the cathode. In contrast, the anodic current densities exhibit only a minor decrease, suggesting a weaker effect on the mild steel dissolution processes.

The observed increase in the cathodic Tafel slopes (Figure 7) suggests that the hydrogen evolution reaction is under activation control. This implies that the inhibitor primarily hinders the reaction by slowing down the initial activation step. The slowdown likely occurs because the adsorbed inhibitor molecules form a monolayer on the mild steel surface, partially blocking the electrolyte from reaching the metal interface and hindering the necessary interactions for hydrogen evolution, as referenced in [11].

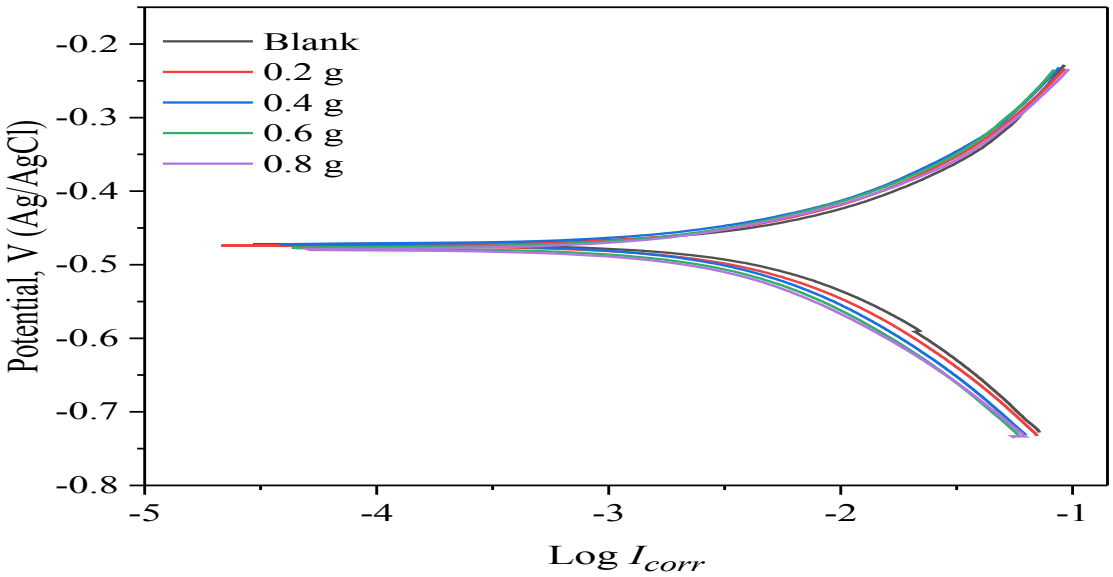

Fig.7: Potentiodynamic polarization curves for mild steel in various concentration with and without (CA) dye.

Table4: Potentiodynamic polarization characteristics for mild steel in various concentration with and without (CA) dye.

Concentration (g L^{-1})	$-E_{corr}$ (mV)	i_{corr} (mA cm^{-2})	β_a (mV dec^{-1})	$-\beta_c$ (mV dec^{-1})	IE (%)
Blank	472.05	108.05	151.87	216.2	-
CA					
0.2	471.45	73.05	146.9	218.42	32.39
0.4	464.82	71.07	914.32	129.74	34.25
0.6	476.4	61.33	163.88	228.04	43.24
0.8	481.05	54.5	132.66	191.88	49.56

Electrochemical Impedance Spectroscopy (EIS)

Electrochemical impedance spectroscopy (EIS) measurements revealed valuable details regarding the mechanism by which the inhibitor hinders corrosion. The Nyquist plot (Figure 8) displays depressed semicircles, indicating a combination of charge transfer and pore resistance processes at the metal-electrolyte interface. Figures 9(a) and 9(b) further illustrate the EIS results. Figure 9(a) shows the phase angle plotted against the logarithm of frequency (log f), while Figure 9(b) presents the Bode modulus (|Z|) versus log f. Key parameters obtained by analyzing this data are summarized in Table 5.

Figure 8 (Nyquist plots) reveals a rising trend in semicircle diameter with increasing inhibitor concentration. This signifies a corresponding increase in charge transfer resistance (Rct), a key indicator of inhibitor effectiveness. Higher R_{ct} values indicate a stronger barrier formed by the inhibitor molecules on the metal surface, hindering corrosion. Additionally, the capacitance of the double layer (C_{dl}) decreases with inhibitor addition, likely due to the formation of a thicker electrical double layer at higher inhibitor concentrations, as reported elsewhere [26].

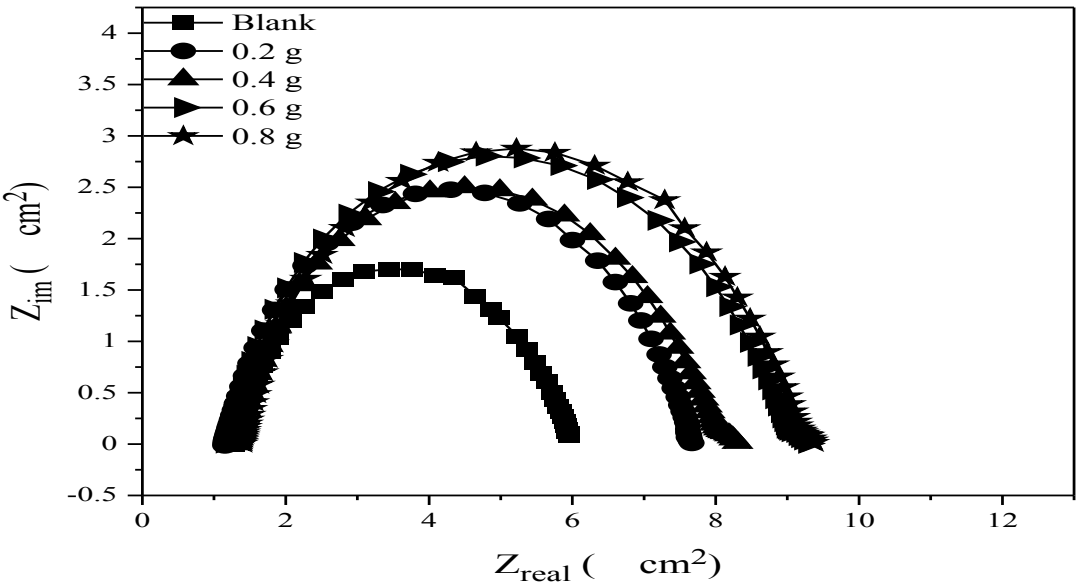

Fig8: Nyquist plot for mild steel corrosion in 1M HCl with and without (CA) dye

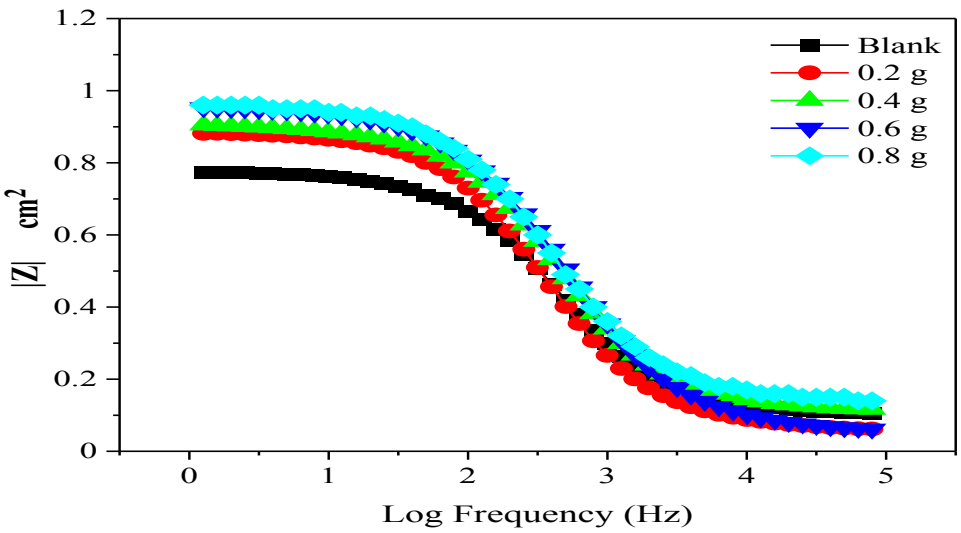

(a)

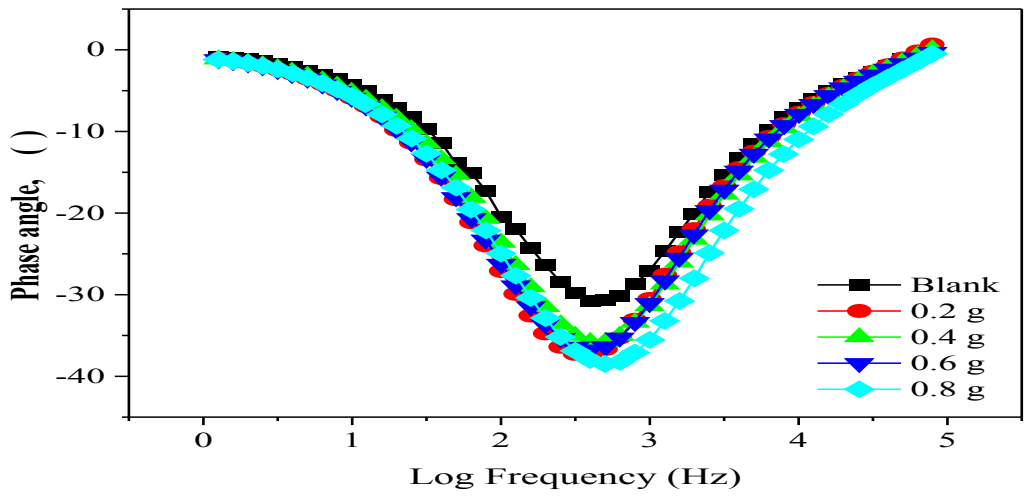

(b)

Fig9(a) and (b): Bode plot for mild steel corrosion in 1M HCl with and without (CA) dye

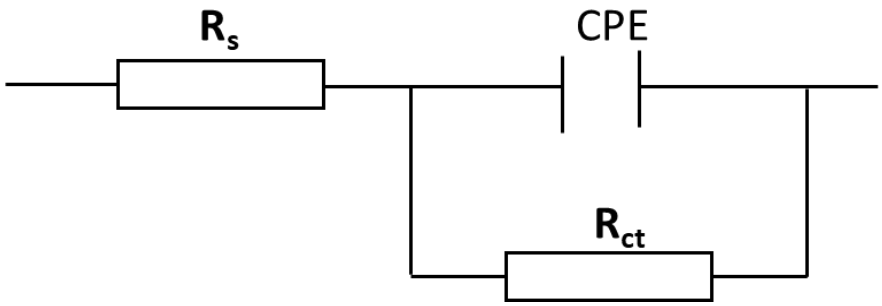

Fig 10: Randle circuit for fitting the EIS data

Table 5: Electrochemical Impedance Spectroscopy characteristics in 1M HCl with and without (CA) dye

Concentration (g L^{-1})	R_s (Ω cm^2)	R_{ct} (Ω cm^2)	Y_o (x 10^{-3} s^n Ω^{-1} cm^{-2})	n	(x 10^6 F cm^2)	IE (%)
blank	2.7458	1.8236	9.202	1.5843	9.8163	-
CA						
0.2	2.9996	2.6548	7.222	1.5744	6.7658	31.31
0.4	3.2936	2.6633	6.618	1.5720	6.0079	31.53
0.6	3.4446	3.1549	6.097	1.5687	5.3004	42.20
0.8	3.6041	3.1773	5.933	1.5676	5.0842	42.61

Surface morphology analysis

Figure 11a shows the SEM image of pristine mild steel for comparison. Figures 11b and 11c depict the surfaces of mild steel submerged in 1 M HCl solutions: one with the CA dye inhibitor (Fig. 11c) and one without (blank solution, Fig. 11b). The extensive surface damage observed in the blank solution (Fig. 11b) indicates significant corrosion compared to the pristine steel (Fig. 11a). This suggests that the CA dye acts as an inhibitor by protecting the metal surface. Figure 11c shows the SEM image of mild steel treated with 1.0 g/L CA dye inhibitor. The surface appears smooth, suggesting minimal corrosion compared to the untreated sample (Fig. 11b). This observation supports the idea that the CA dye inhibitor effectively protects the metal surface.

Energy-dispersive X-ray spectroscopy (EDX) analysis of iron weight concentration further supports the protective effect of the CA dye inhibitor at a concentration of 1.0 g/L. This aligns with the findings from scanning electron microscopy (SEM) images (Fig. 11), which show a smoother surface in the presence of the inhibitor compared to the untreated sample. Both EDX and SEM analyses indicate that the CA dye effectively shields the mild steel surface from corrosion in 1 M HCl solution. These observations are consistent with the results obtained from other techniques, such as electrochemical measurements and weight loss studies.

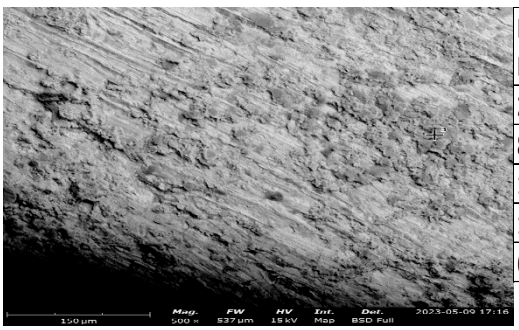

Element Number	Element Symbol	Element Name	Atomic Conc.	Weight Conc.
26	Fe	Iron	57.83	93.37
8	O	Oxygen	22.17	10.81
12	Mg	Magnesium	4.29	2.59
14	Si	Silicon	3.61	2.52
6	C	Carbon	1.71	0.51

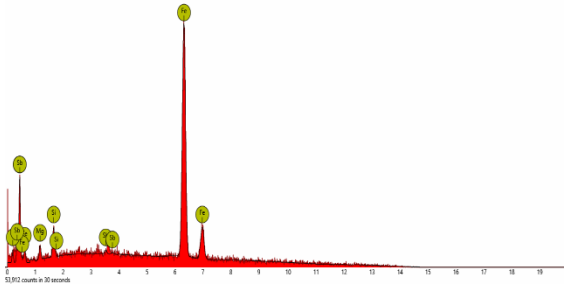

Fig 11(a):SEM image and EDX analysis of plain pristine mild steel

Element Number	Element Symbol	Element Name	Atomic Conc.	Weight Conc.
8	O	Oxygen	57.42	47.10
14	Si	Silicon	16.15	23.25
12	Mg	Magnesium	15.11	18.82
7	N	Nitrogen	7.96	5.72
6	C	Carbon	2.01	1.24
26	Fe	Iron	1.35	3.87

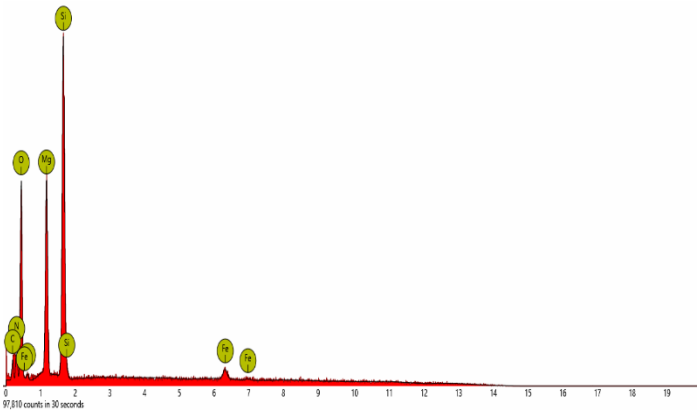

Fig11(b):SEM image and EDX analysis of mild steel after immersion in 1M HCl Blank solution

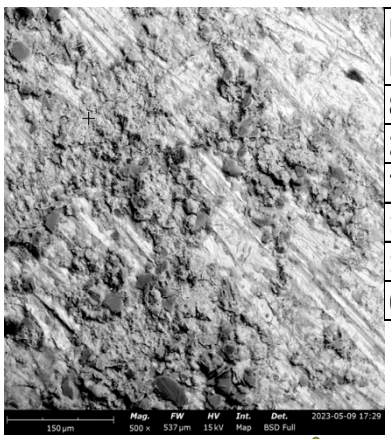

Element Number	Element Symbol	Element Name	Atomic Conc.	Weight Conc.
8	O	Oxygen	42.19	27.62
26	Fe	Iron	24.10	51.49
7	N	Nitrogen	7.72	4.14
12	Mg	Magnesium	4.27	3.97
14	Si	Silicon	3.50	3.76
6	C	Carbon	2.22	1.02

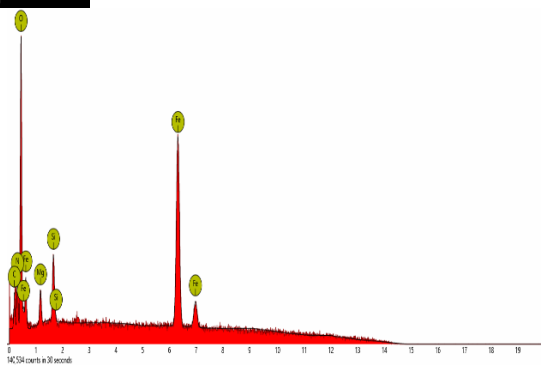

Fig11(c): SEM image and EDX analysis of Mild steel after immersion into *CA* dye inhibitor solution

Table 6: SEM-EDX parameters for mild steel corrosion in 1MHCl in the absence and presence of dye extracts

Samples	Weight Conc.	Difference In Weight Conc.	Percent. Difference in Weight Conc
Plain pristine Mild Steel	93.37	-	-
Mild Steel + 1M HCl	3.87	89.50	95.86
Mild Steel + *CA dye*	51.49	41.88	44.85

GC -MS and HPLC ANALYSIS

GC-MS ANALYSIS RESULTS FOR *Cola acuminata*

Pk NO	RT	Area%	Library/ID	Ref NO	CAS NO	Qual
1	3.591	0.84	Furan, 2,5-dimethyl-	3113	000625-86-5	46
2	5.651	0.51	Cyclopentane, 1-ethyl-3-methyl-, trans-	7560	002613-65-2	43
3	6.566	93.54	Caffeine	65390	000058-08-2	97
4	6.755	1.10	Theobromine	52456	000083-67-0	97
5	7.030	1.26	n-Hexadecanoic acid	129145	000057-10-3	96
6	7.156	0.68	Hexadecanoic acid, ethyl ester	159424	000628-97-7	97
7	7.928	0.70	8-Hexadecyne	93953	019781-86-3	86
8	7.974	0.77	cis-Vaccenic acid	156903	000506-17-2	91
9	8.088	0.60	Ethyl Oleate	187619	000111-62-6	98

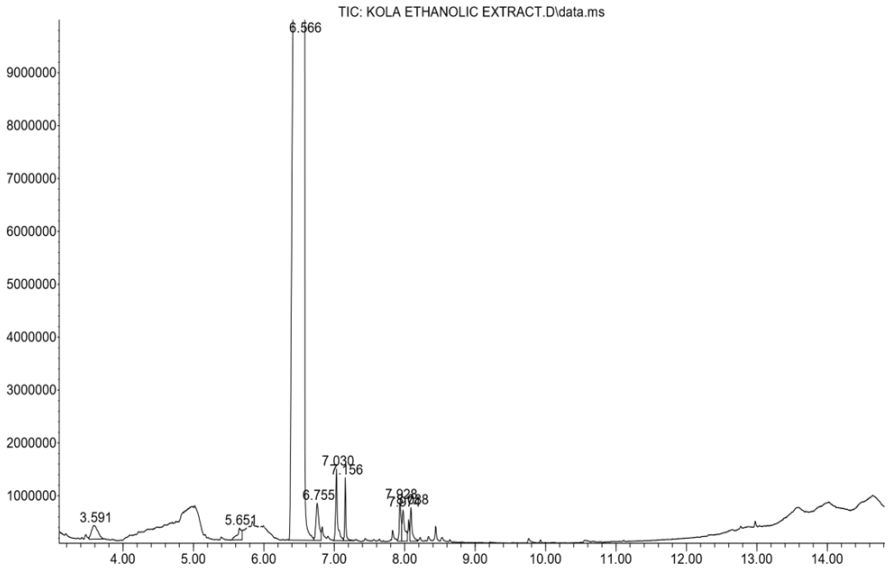

HPLC ANALYSIS RESULTS FOR *Cola acuminata*

S/N	Retention Time [min]	Compound Name	Concentration mg/L
1	12.291	Naringin	6.642
2	16.188	Myricetin	4.312

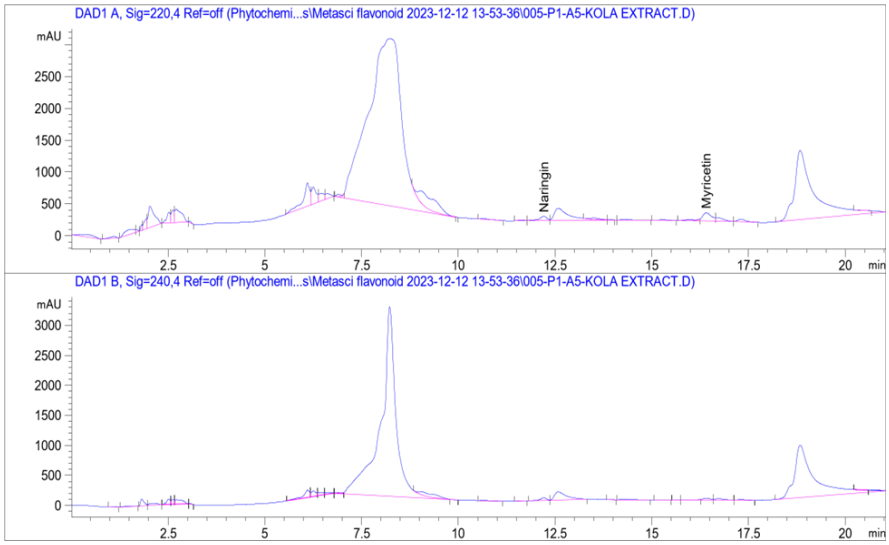

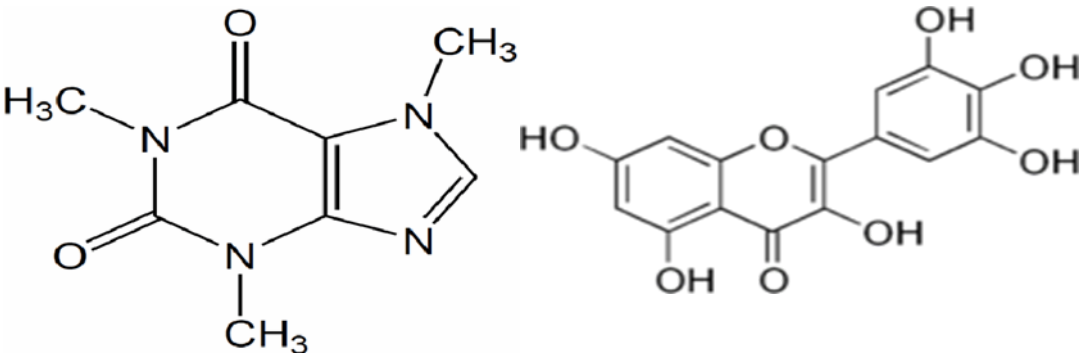

Caffeine **Myricetin.**

Analysis by GC-MS identified 9 bioactive compounds in the CA dye extract with Caffeine being the most abundant.HPLC analysis revealed the presence of Naringin, and Myricetin. Notably, Myricetin was identified as a common bioactive phytochemical present in the leaf extract of CA. [27-28]

COMPUTAIONAL AND QUANTUM STUDIES

Computational Analysis

Comparison of computational UV/Visible and IR spectra with experimental data reveals similar absorption bands in the UV/Visible region (200-400 nm) [29] and similar functional groups (-OH, -CH, C=C, and C=O) in the IR region. This is consistent with the experimental findings for UV/Visible and IR spectroscopy [29, 15].

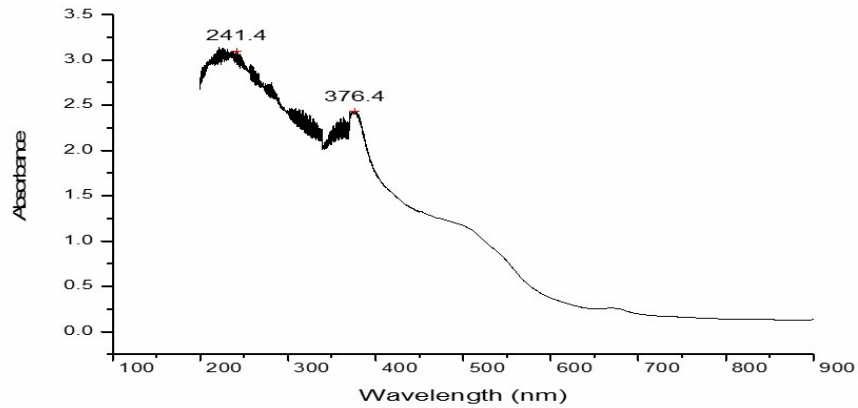

(a)

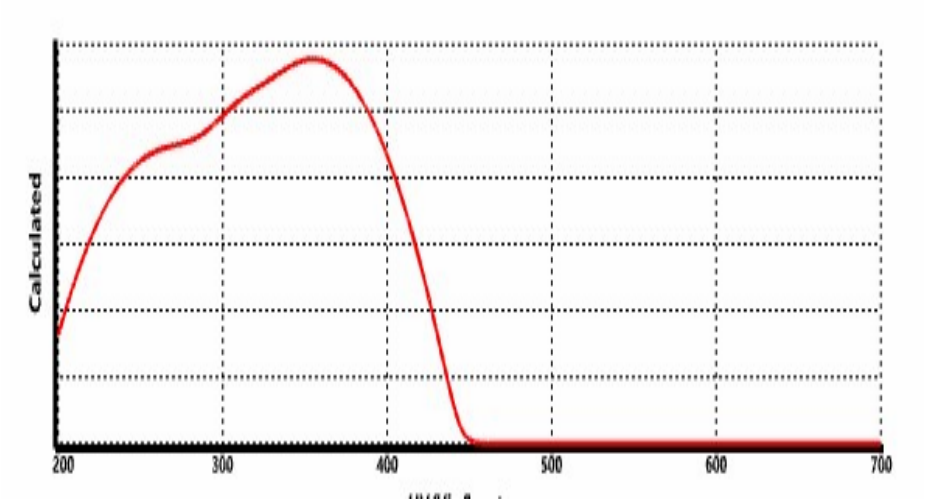

(b)

Fig12: UV–Vis absorption spectrum of (a) Experimental (b) Computational

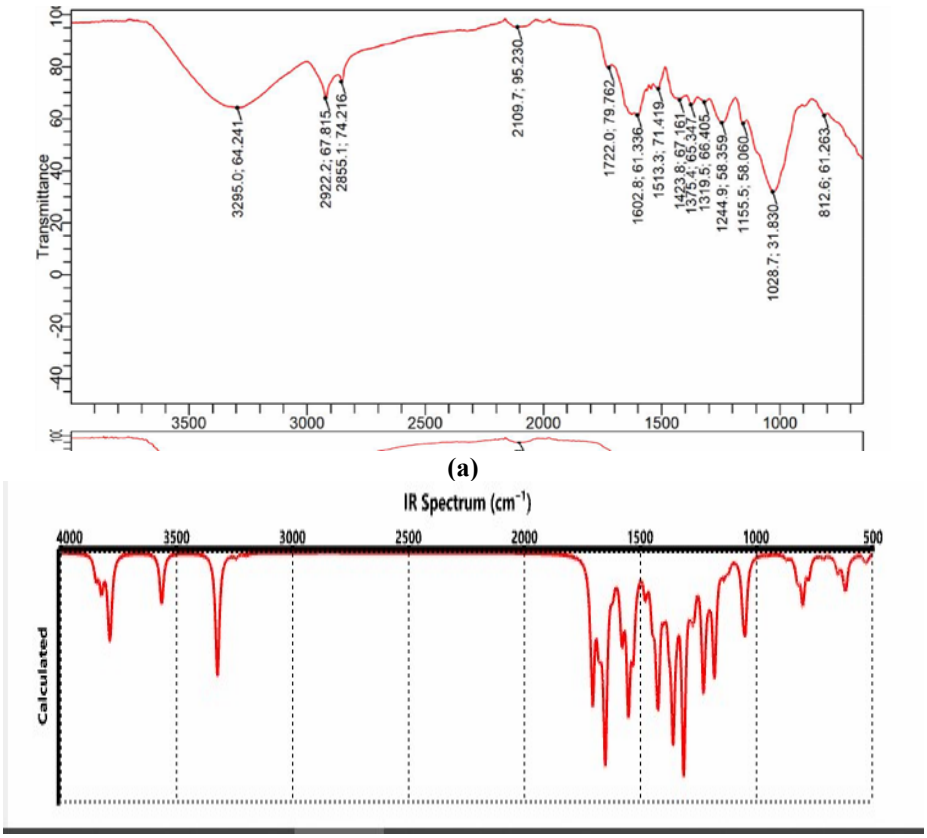

(a)

(b)

Fig 13: IR spectrum of (a) Experimental (b) Computational

Quantum Chemical Studies

DFT/B3LYP is a powerful tool for calculating various molecular properties. DFT/B3LYP calculations reveal key properties that influence how molecules interact (Table 6). These properties include: HOMO and LUMO energies: These indicate a molecule's tendency to donate (HOMO) or accept (LUMO) electrons; Energy Gap: This reflects the energy difference between donating and accepting an electron; Dipole Moment: This measures a molecule's electrical polarity; Electron Affinity (EA) and Ionization Potential (IP): These describe how easily a molecule gains or loses an electron, respectively; Hardness and Softness: These quantify a molecule's resistance to electron donation (hardness) or acceptance (softness). Crucially, interactions between the HOMO of one molecule and the LUMO of another are considered essential in this theory. A molecule with a high HOMO energy is more likely to donate an electron.

Higher HOMO values indicate a greater likelihood of electron donation to other molecules with empty orbitals (acceptors). Corrosion inhibitors can act in two ways The inhibitor acts like a double agent with the metal surface: (1) Electron Donor: It can donate electrons to the empty d-orbitals of metal ions, partially filling them. (2) Electron Acceptor: Conversely, it can also accept electrons from the filled d-orbitals of the metal

Myricetin's effectiveness as a corrosion inhibitor stems from its ability to both donate and accept electrons. The calculated HOMO energy (EHOMO) value of -5.46 eV indicates a strong tendency for Myricetin to donate electrons, which is a desirable trait for corrosion inhibitors. Myricetin's talent for both donating and accepting electrons likely explains its effectiveness as a corrosion inhibitor [30]. Here's why: Electron Donor: Its high HOMO energy (energy of the highest occupied molecular orbital) indicates a strong tendency to donate electrons. This is often linked to good corrosion inhibition performance. Electron Acceptor: The low ELUMO value (energy of the lowest unoccupied molecular orbital, (-1.83 eV) suggests Myricetin can also readily accept electrons. This dual ability to give and take electrons might be key to Myricetin's superior performance.

The gap between the HOMO and LUMO energies, known as ΔE (Delta E), plays a critical role in how inhibitor molecules interact with the metal surface. This difference is called the energy gap. When the energy gap (ΔE) is smaller, the inhibitor molecule is generally considered more reactive. This increased reactivity can lead to stronger adsorption on the metal surface. Based on the calculations in Table 6 , Myricetin appears to have the lowest energy gap among the studied molecules. Myricetin's lower HOMO-LUMO energy gap (ΔE) suggests it could be more reactive and potentially adhere (adsorb) more effectively to the metal surface. This stronger interaction might be why Myricetin performs better at inhibiting corrosion [31].

The dipole moment (μ) tells us how unevenly charged a molecule is. Some studies suggest a high dipole moment might improve an inhibitor's ability to stick to the metal surface (adsorption) [32]. However, other research contradicts this, indicating that lower dipole moments might be more favorable for adsorption [33]. In this study, Myricetin has a lower dipole moment compared to Caffeine molecules. The influence of dipole moment on adsorption in this specific case remains unclear and requires further investigation.

Ionization energy (I) refers to the energy needed to remove the easiest electron from a molecule in its gaseous form. Molecules with lower ionization energy (I) tend to lose electrons more readily. This makes them generally more reactive and better reducing agents [34]. The calculations show that Myricetin has a low ionization energy compared to other studied molecules. This suggests Myricetin might be more reactive, which could contribute to its effectiveness as a corrosion inhibitor. Electron affinity (EA) tells us how much energy is released when a molecule gains an electron [35]. A high electron affinity for Myricetin suggests it could readily accept electrons from the metal surface. This potential electron acceptance might contribute to its corrosion inhibition efficiency. Electronegativity describes an atom's attraction for electrons in a bond. Some studies suggest highly electronegative molecules might be less reactive, leading to lower corrosion inhibition [36]. In this case, both Myricetin and Caffeine have relatively low and similar electronegativity values. This study considers absolute hardness, which relates to a molecule's stability and resistance to change. Harder molecules have larger energy gaps, while softer molecules have smaller gaps. The calculations suggest Myricetin has a lower hardness value and a smaller energy gap compared to other studied molecules. This indicates Myricetin might be softer and more reactive, which could contribute to its effectiveness as a corrosion inhibitor [29].

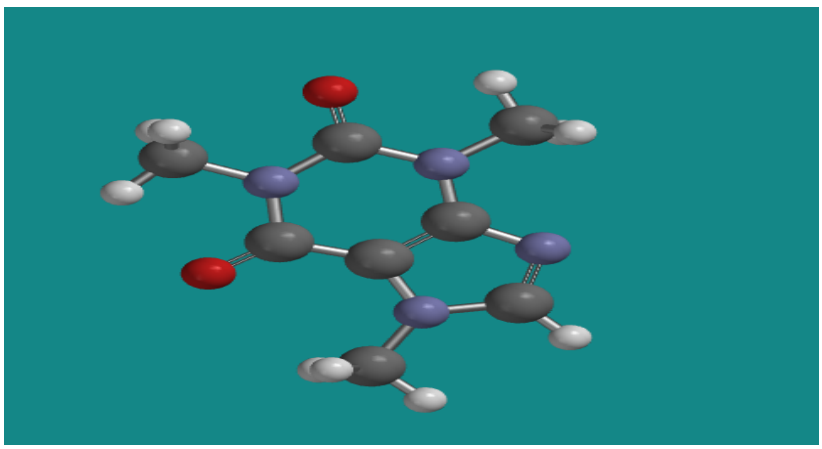

Fig 14: (a) Optimized Geometry of Caffeine Structure

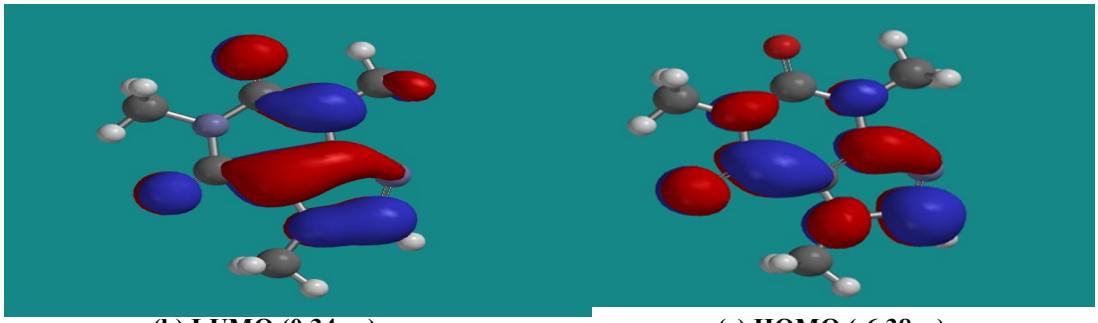

(b) LUMO (0.34 ev) **(c) HOMO (-6.38ev)**

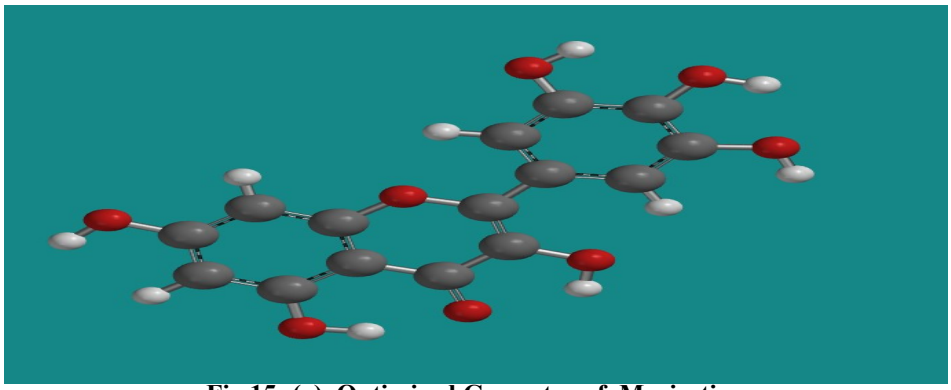

Fig 15: (a) Optimized Geometry of Myricetin

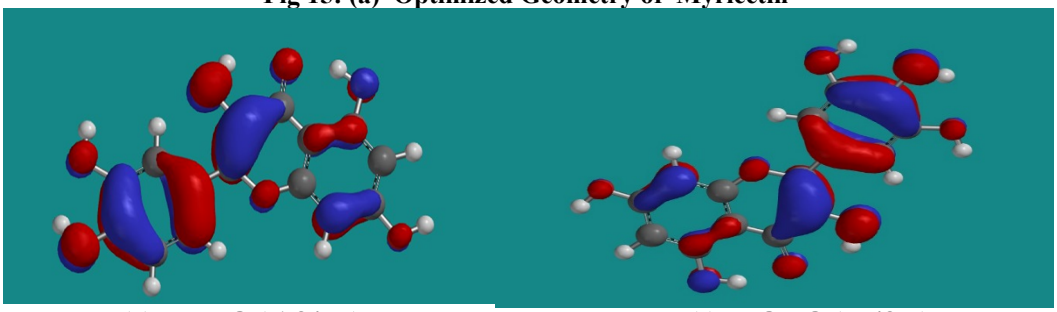

(b) LUMO (-1.84 ev) **(c) HOMO (-5.48ev)**

Table 6: Quantum parameters for *(CA)* dye

S/N	Parameters	**Caffeine**	**Myricetin**
1	E_{HOMO} (ev)	-5.97	-5.46
2	E_{LUMO} (ev)	-0.86	-1.83
3	Energy Gap (ΔE) (ev)	5.11	3.64
4	Ionisation potential (IP)	5.97	5.46
5	Electron Affinity (EA)	0.86	1.83
6	Diapole Moment	3.76	1.54
7	Absolute Hardness (η)	2.56	1.82
8	Absolute Softness (σ)	0.39	0.55

IV. Conclusion

The extract worked better at preventing corrosion as more was added to it. This suggests a thicker protective layer coating the metal at higher concentrations. Inhibition efficiency decreased with higher temperatures. This is likely because the inhibitor requires more energy (activation energy) to be effective at higher temperatures. The negative values of ΔH^0 (enthalpy change) indicate the corrosion inhibition process absorbs heat (endothermic). The negative value of ΔG ads, the free energy change of adsorption, indicates that the inhibitor molecules spontaneously bond, or adsorb, to the metal surface. This suggests a favorable interaction between the inhibitor and the metal. The adsorption process itself likely follows the Langmuir isotherm model, a well-established model for describing how a single layer of molecules forms (monolayer adsorption) on a surface. Analysis of the extract identified caffeine and myricetin as key components. Quantum chemistry calculations predicted that Myricetin, in particular, would have superior inhibition properties within the extract. The excellent agreement between theory (quantum chemistry) and practice (experiments) paves the way for designing even more effective corrosion inhibitors using computational methods

REFERENCES

[1]. Asafa ,T.B, Odusote, J.K, Ibrahim, O.S , Lateef, A, Durowoju, M.O, Azeez, M.A, Yekeen,T.A, Oladipo, I.C, Adebayo ,E.A, Badmus, J.A, Sanusi, Y.K. & Adedokun, O .steel, stainless steel and aluminum in 1.0 M HCl
medium *IOP Conf. Series: Materials Science and Engineering* 805, (2020).1-17

[2]. Ismail, A .A Review of green corrosion inhibitor for mild steel in Seawater, *ARPN Journal of Engineering and Applied Sciences* . 11(14), (2016),8710-8714

[3]. Peme, T., Olasunkanmi, L.O., Bahadur, I., Adekunle, S., Kabanda, M.M. & Ebenso, E.E.Adsorption and Corrosion Inhibition Studies of Some Selected Dyes as Corrosion Inhibitors for Mild Steel in Acidic Medium: Gravimetric, Electrochemical, Quantum Chemical Studies and Synergistic Effect with Iodide Ions, *Molecules*, 20 , (2015),16004-16029.

[4]. Godwin, A.I., Surma, N. & John, O.I. Ag-nanoparticles Mediated by *Lonchocarpus laxiflorus Stem Bark* Extract as Anticorrosion Additive for Mild Steel in 1.0 M HCl Solution, *Progress in Chemical and Biochemical Research* , 5(2), (2022),133-146

[5]. Efe, M. O., Stephen, A. J. & Asefon, O. A. The Phytochemical Properties and Antimicrobial Potentials of Aqueous and Methanolic seed Extract of Cola nitida (Vent.) and *Cola acuminata*(Beauvoir) grown in South West, Nigeria Saudi J. Med. Pharm. Sci., 2 (12), (2016),354-363

[6]. Abdul-Rashid, I. M., Moses, M.S., Kabiru, H., Saviour, A. U. & Tawfik, A S. Evaluation of the corrosion inhibition efficacy of *Cola acuminata* extract for low carbon steel in simulated acid pickling environment , *Environ Sci Pollut. Res. Int .,* 27(27), (2020),34270-34288.

[7].Pratap, R., Manthur, P., Ramchander, M., Rama, K., Veera, B.N. & Raju, N. Biogenic Synthesis of Silver Nanoparticles Using *Tectona grandis* Leaf Extract and evaluation of theirAntibacterial Potential, *International Journal of ChemTech Research,* 6, (1) , (2014),293-298.

[8]. Khalid, S., Shahzad, A., Basharat, N., Abubakar, M. & Anwar, P. Phytochemical Screening and Analysis of Selected Medicinal Plants in Gujrat. *J Phytochemistry Biochem* 2, (2018),108.

[9]. Seema, K. & Jaya, M. Extraction, Phytochemicals Screening and Antibacterial activity of Carica papaya Leaf Extracts,*Der Pharma Chemica*, 12(5), (2020), 41-47.

[10], Olasehinde, E.F., Agbaffa, B.E. Adebayo, M.A. & Enis, J, Corrosion protection of mild steel in acidic medium by titanium-based nanocomposite of *Chromolaena odorata* leaf extract *Materials Chemistry and Physics*, 281, (2022), 1-10

[11]. Filali Baba, Y. Elmsellem , H. Kandri Rodi1 , Y , Steli , H ,Ouazzani Chahdi , F , Ouzidan. Y, Sebbar , N. K, Essassi, E. M, El-Hajjaji , F & Hammouti, B. Experimental and quantum chemical studies on corrosion inhibition effect of 6-bromo-2-oxo-1,2-dihydroquinoline-4-carboxylic acid on mild steel in HCl Solution, *Der Pharmacia Lettre*,, 8 (10),(2016),128-137

[12]. Kanoma A. I., Muhammad, I., Abdullahi, S., Shehu, K., Maishanu, H. M.& Isah, A. D.Qualitative and Quantitative Phytochemical Screening of Cola Nuts (*Cola Nitida And Cola acuminata*) *Journal of Biology, Agriculture and Healthcare* ,4, (2014),(5),89

[13]. Mabasa, X. E., Mathomu, L. M., Madala, N. E., Musie, E. M. & Sigid, M. T. Molecular Spectroscopic (FTIR and UV-Vis) and Hyphenated Chromatographic (UHPLC TOF-MS). Analysis and In Vitro Bioactivities of the *Momordica balsamina* Leaf Extract. *Biochemistry Research International,* 2021, 1-12

[14].Patle, T. K., Shrivas, K., Kurrey, R., Upadhyay, S., Jangde, R. & Chauhan, R.Phytochemical screening and determination of phenolics and flavonoids in *Dillenia pentagyna* using UV-vis and FTIR spectroscopy, *Spectrochimica Acta Part A: Molecular and Biomolecular Spectroscopy*, (2020),242.

[15] Emeka, E.E., Ojiefoh, O.C., Aleruchi, C., Hassan, L.A., Christiana , O.M., Rebecca, M.,Dare, E.O. & Temitope, A.E. Evaluation of antibacterial activities of silver nanoparticles green-synthesized using pineapple leaf (*Ananas comosus*), *Micron* ,57, (2014),1–5.

[16]. Shankar, S., Jaiswal, L., Aparna, R.S.L. & Prasad, R.G.S.V. Synthesis, characterization,in vitro biocompatibility, and antimicrobial activity of gold, silver and gold silver alloy nanoparticles pre-pared from *Lansium domesticum* fruit peel extract, *Mater. Lett*.,137, (2014),75–78

[17]. Agbaje, L, Musibau, A. A., Tesleem, B. A., Taofeek, A. Y., Akeem, A., Iyabo, C. O., Luqmon, A., Sadiat, E. A., Sunday, A. O., Evariste, B. G. & Lorika, S. B. Biogenic synthesisof silver nanoparticles using a pod extract of *Cola nitida*: Antibacterial and antioxidant activities and application as a paint additive, *Journal of Taibah University for Science,* 10, (2016),551–562

[18].Sanatkumar, B.S., Nayak, J. & Nityananda Shetty, A. Influence of 2-(4-chlorophenyl)- 2-oxoethyl benzoate on the hydrogen evolution and corrosion inhibition of 18 Ni 250 grade weld aged maraging steel in 1.0 M sulfuric acid medium, *Int. J. Hydrogen Energy*, 37, (2012),9431–9442,

[19]. Odewunmi, N.A, Umoren, S.A. & Gasem, Z.M. Watermelon waste products as green corrosion inhibitors for mild steel in HCl solution.,*J. Environ. Chem. Eng.* 3(1) (2015),286-296.

[20].Oguzie, E. E. Studies on the inhibitive effect of *Occimum viridis* extract on the acid corrosion of mild steel," *Journal of Materials chemistry and physics*, 99, (2-3) , (2006), 441–446

[21]. Egbeneje, V.O., Okhale, S .E., Moisi, C, Ogbogo, I.O. & Ojo, O. Evaluation of the Inhibitive Properties of Silver Nanoparticles in *Senna occidentalis* Root Extract as Corrosion Inhibitor ofMild Steel, *Tanzania Journal of Science* 49(3), (2023),655-663

[22]. Kandregula, C., Chinthakuntla, A., Rao, K. & Rajendar, V. (2014). Green synthesis of TiO_2 nanoparticles using Hibiscus flower extract, *Int. Conf. Emerg. Technol. Mech*. Sci.2, 79–82.

[23]. Umoren, S.A. and Solomon, M.M. (2015). Performance assessment of poly (methacrylic acid) silver nanoparticles composite as corrosion inhibitor for aluminium in acidic environment, *Adhes. Sci.Technol*., 9, 2311–2333,

[24]. Eddy, N.O. & Ebenso, E.E. Adsorption and inhibitive properties of ethanol extract of *Musa sapientum* peels as a green corrosion inhibitor for mild steel in H_2SO_4. *Afr. J. Pure Appl .Chem*. 2(6), (2008).,46-54.

[25]. Muthukrishnan, P., Jeyaprabha, B. & Prakash, P. Adsorption and corrosion inhibiting behavior of *Lannea coromandelica* leaf extract on mild steel corrosion, *Arab. J. Chem*., 10, (2017) ,2343–2354

[26]. Kathirvel, K. Thirumalairaj, B. & Jaganathan, M. Quantum Chemical Studies on the Corrosion Inhibition of

Mild Steel by Piperidin-4-One Derivatives in 1 M H_3PO_4. *Open Journal of Metal*, 4, (2014) , 73-85.

[27]. Blaise M. M, Clément L. I, Jean-Jacques O. A,Colette M.A, Jonas M.S. N, Pius T. M Koto-Te-Nyiwa N .

Mini-review on the phyto-chemistry, pharmacology and toxicology of *Cola nitida* (Vent.) Schott & Endl.

(Malvaceae): A medically interesting bio-resource of multiple purposes in Africa, *Natr Resour Human*

Health 2 (3), (2022) , 335-342

[28]. Adesanwo J K,.Ogundele S B, Akinpelu D A. &McDonald A G. Chemical Analyses,Antimicrobial and

Antioxidant Activities of Extracts from *Cola nitida* Seed, Journal of Exploratory Research in Pharmacology

vol. 2,(2017) 67–77

[29]. Naira, N., & Karvekar, M. D. Isolation of phenolic compounds from the methanolic extract of *Tectona grandis*. *Research Journal of Pharmaceutical Biological and Chemical Sciences, 1*(2), (2010),221-225

[30]. Zarrouk A,. El Ouali I, Bouachrine M., Hammouti B , Ramli Y, Essassi , E. M.. Warad, I, Aouniti , A & Salghi, R .Theoretical approach to the corrosion inhibition efficiency of some quinoxaline derivatives of steel in acid media using the DFT method ,*Res Chem Intermed*, (2012).

[31] .Lebrini, M , Lagrenée, M, Vezin, H , Traisnel , M & Bentiss F. Experimental and theoretical study for corrosion inhibition of mild steel in normal hydrochloric acid soluti by some new macrocyclic polyether compounds. *Corrosion Science*, 49, (2007),2254- 2269.

[32]. Khaled. K. F. Molecular simulation, quantum chemical calculations and electrochemical studies inhibition of mild steel by triazoles. *Electrochimica Acta,* , 53, (2008),3484-3492.

[33].Wazzan .N. A. & Mahgoub. F.M.DFT Calculations for Corrosion Inhibition of FerrousAlloys by Pyrazolo pyrimidine Derivatives. *Open Journal of Physical Chemistry*, 4, (2014), 6-14.

[34]. Obi-Egbedi N. O. & Obot I. B. Inhibitive properties, thermodynamic and quantum.chemical studies of Alloxazine on Mild steel corrosion in H_2SO_4. *Corrosion Science*, 53,(2011),263-275.

[35]. Saranya J., Sounthari P, Paranswari K. &Chitra S. Adsorption and density functional theory on Corrosion

of mild steel by a quinoxaline derivative. *Der Pharma Chemica*, 8, (2015), 187-196.

[36]. Geerlings P & De Proft F .Chemical reactivity as described by quantum chemical methods. *International Journal of Molecular Sciences*, 3, (2002), 276-309.